Experimental Search on the QCD Critical Point

Yu Zhang[1,*]

[1]Guangxi Normal University, Guilin, 541006, China

Abstract. The QCD critical point is a landmark on the QCD phase diagram, attracting much effort to confirm its location. In these proceedings, we present recent experimental progress in the search for the QCD critical point. The results, comparisons with models, and implications for the QCD critical point will also be discussed.

1 Introduction

The QCD critical point (CEP) is predicted to be the end point of the first-order phase transition boundary between the Quark-Gluon Plasma (QGP) and hadron gas on the QCD phase diagram. Much effort has been made to look for it from both theory and experiment. In these proceedings, we show recent progress from experiment on the search for the QCD critical point.

2 Intermittency Analysis

Intermittency is used to look for the critical behavior induced by the critical point in heavy-ion collisions [1]. In the vicinity of CEP, the correlation length of the system diverges, and the system turns to be self-similar. Based on the 3D-Ising universality class, the density-density correlation function for small momentum transfer has a power-law structure, which leads to large density fluctuations. Intermittency analysis can capture these fluctuations using scaled factorial moments in transverse momentum space. qth-order scaled factorial moments are defined by Eq. (1) where M^D is the number of cells in D-dimensional phase space and n_i is the measured multiplicity of a given event in the ith cell. Two types of power-law behavior are shown as $F_q(M) \propto (M^D)^{\phi_q}$ and $F_q(M) \propto F_2(M)^{\beta_q}$, separately, where ϕ_q and β_q are called intermittency index and scaling index. According to Ginzburg-Landau theory, the β_q follows $\beta_q \propto (q-1)^{\nu}$ and is predicted to be 1.034, which is 1.0 in 2D-Ising model calculation.

$$F_q(M) = \frac{\langle \frac{1}{M^D} \sum_{i=1}^{M^D} n_i(n_i-1)\cdots(n_i-q+1)\rangle}{\langle \frac{1}{M^D} \sum_{i=1}^{M^D} n_i\rangle^q} \tag{1}$$

Figure 1 shows $\Delta F_q(M)$ ($q > 2$, $F_q(M)$ after background subtraction) up to sixth-order of identified charged hadrons as a function of second-order $\Delta F_2(M)$ in 0-5% central Au+Au collisions at $\sqrt{s_{NN}}$ = 7.7 - 200 GeV [2]. The black solid lines indicate linear fitting to data. The power-law structure of $F_q(M) \propto F_2(M)^{\beta_q}$ are clearly seen in each energy. The power

*e-mail: zhangyu@gxnu.edu.cn

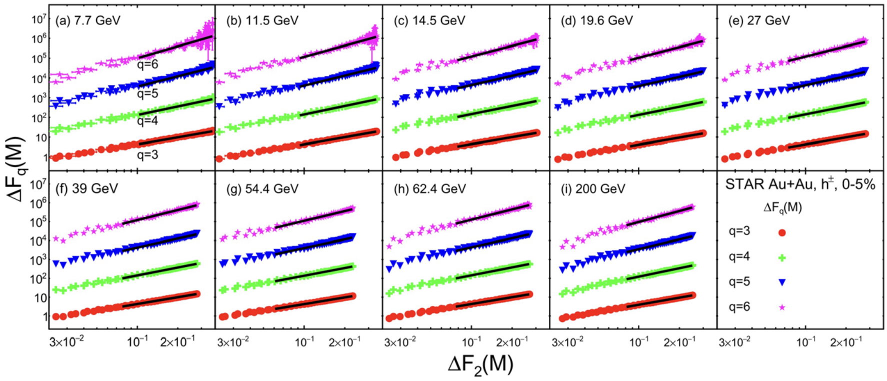

Figure 1. $\Delta F_q(M)$ as a function of $\Delta F_2(M)$ in most central Au+Au collisions at $\sqrt{s_{NN}}$ = 7.7-200 GeV. The solid black lines represent the best power-law fit of $\Delta F_q(M) \propto \Delta F_2(M)^{\beta_q}$.

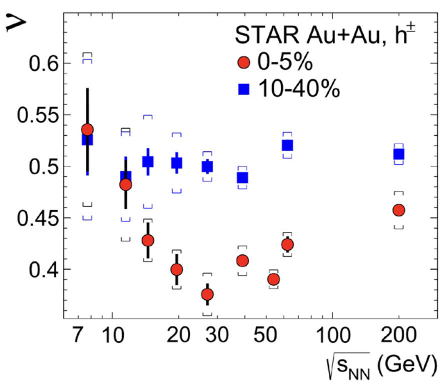

Figure 2. Energy dependence of the scaling exponent (ν) for identified charged hadrons ($h^{\pm}$) in Au+Au collisions at $\sqrt{s_{NN}}$ = 7.7-200 GeV.

series β_q is then extracted from each energy. In agreement with theoretical expectation, β_q obeys a power-law behavior with $q-1$. The scaling exponent ν can be obtained through a power-law fitting on $\beta_q \propto (q-1)^{\nu}$. Figure 2 shows the energy dependence of β_q for identified charged hadrons in 0-5% central and 10-40% mid-central Au+Au collisions. In 5% most central collisions, ν exhibits a non-monotonic behavior as a function of collision energy and reaches a minimum at around $\sqrt{s_{NN}}$ = 27 GeV. In contrast, ν shows flat energy dependence in 10-40% mid-central collisions. The observed non-monotonic energy dependence of ν in 0-5% most central collisions could be due to the signal of density fluctuations induced by the QCD critical point. The measured ν in Fig. 2 is smaller than the theoretical calculation of the critical ν = 1.30 by the Ginzburg-Landau theory. However, the theoretical calculation is performed over an entire phase space while the data is measured within limited η and p_T acceptance. Theoretical calculations implemented in a limited transverse momentum phase space and equivalent experimental acceptance, are necessary to understand the measurements.

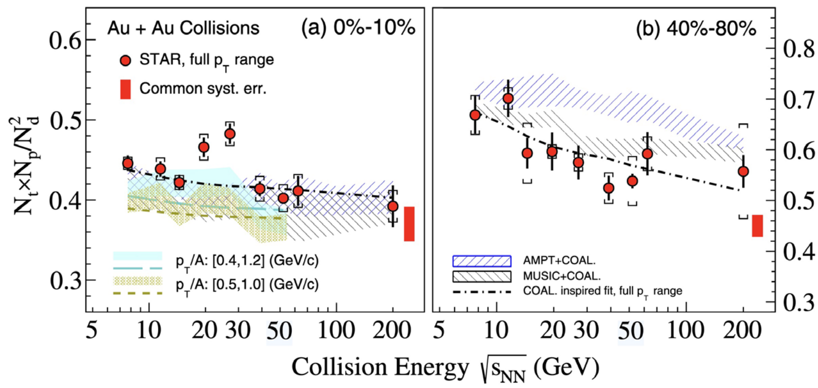

Figure 3. Collision energy, centrality, and p_T dependence of the yield ratio $N_t \times N_p/D_d^2$ in Au+Au collisions at RHIC. Solid circles are the results from 0–10% central (left panel) and 40–80% peripheral (right panel) collisions.

3 Light Nuclei Yield Ratio

The production of light nuclei like deuteron, triton, and helium-3 provides important information on nuclear matter at high baryon density and temperature. It is proposed by the coalescence model [3] that the compound yield ratio $N_t \times N_p/N_d^2$ of tritons (N_t), deuterons (N_d), and protons (N_p) is sensitive to neutron density fluctuations, making it a promising observable for the QCD critical point. Below we show recent progress from RHIC-STAR experiment.

Figure 3 shows the energy dependence of the yield ratio $N_t \times N_p/N_d^2$ at mid-rapidity in 0-10% central and 40-80% peripheral Au+Au collisions at $\sqrt{s_{NN}}$ = 7.7 - 200 GeV [4]. For comparisons, the calculations of AMPT, MUSIC+UrQMD hybrid models are shown in shaded areas. For 0-10% most central Au+Au collisions, the yield ratios are consistent with the coalescence baseline and model calculation, except for the enhancements of the yield ratios to the coalescence baseline with a significance of 2.3σ and 3.4σ observed at $\sqrt{s_{NN}} = 19.6$ and 27 GeV, respectively. In peripheral collisions, similar to data, model calculations have a smooth decreasing trend as a function of collision energy. If the enhancements in 0-10% central collisions are due to large baryon density fluctuations near the critical point, further theoretical studies are needed, especially the dynamical modeling of heavy-ion collisions with a realistic equation of state.

4 Baryon-strangeness Correlation

Baryon-strangeness correlation is proposed to be a diagnostic of the degree of freedom and correlations of strongly interacting matter. It could be used to identify the onset of deconfinement [5]. The definition of the baryon-strangeness correlation is $C_{BS} = -3\frac{\langle BS\rangle - \langle B\rangle\langle S\rangle}{\langle S^2\rangle - \langle S\rangle^2}$, where B and S indicate number of baryon and strangeness, respectively. For QGP, if quark flavors are uncorrelated, then the C_{BS} ratio is unity. While for hadron gas, the C_{BS} depends on hadron environment. The estimation of C_{BS} in the statistical model for a hadron resonance

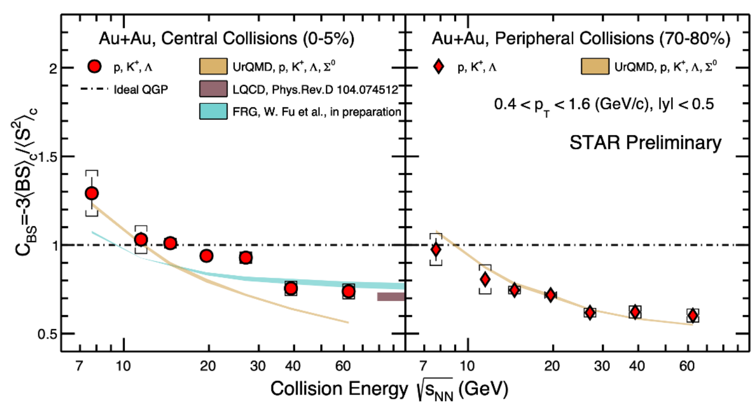

Figure 4. Collision energy dependence of the baryon-strangeness correlation C_{BS} in 0-5% and 70-80% Au+Au collisions.

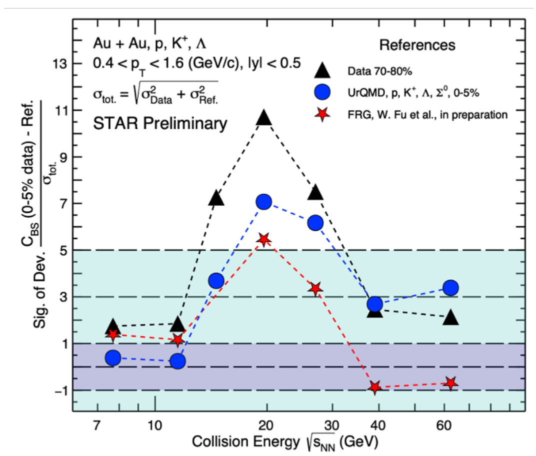

Figure 5. Collision energy dependence of deviation of C_{BS} ratio from peripheral data, UrQMD and FRG model calculations.

gas model at zero baryon chemical potential Here, we show recent measurements on baryon-strangeness correlation in Au+Au collisions at $\sqrt{s_{NN}}$ = 7.7 - 62.4 GeV from RHIC-STAR. Particles in measurements include (anti)proton, $K^{\pm}$, and Λ ($\bar{\Lambda}$).

Figure 4 shows the energy dependence of C_{BS} ratio in Au+Au collisions at $\sqrt{s_{NN}}$ = 7.7 - 62.4 GeV for 0-5% and 70-80% centrality. The data points are shown with red circles, while colored bands represent model calculations from UrQMD, LQCD, and FRG. The experimental measurements are done within $|y| < 0.5$ and $0.4 < p_T < 1.6$ GeV/c. The data in peripheral collisions are qualitatively consistent with calculation from the UrQMD model, while in 0-5% central collisions, the data show deviations from various model calculations. The deviations as a function of collision energy between data from central collisions and peripheral collisions and model calculations are shown in Fig. 5. It can be seen that the deviation reaches a maximum at 19.6 GeV. The physics behind this discrepancy needs further investigation.

5 Net-proton Cumulants

Cumulants of conserved quantities like net-baryon, net-charge, and net-strangeness number are proposed as sensitive observables [6] to the QCD critical point and have been studied extensively both in experiment and theory.

Recently, preliminary results of net-proton cumulants on STAR BES-II datasets are available. This measurement is performed in Au+Au collisions at $\sqrt{s_{NN}}$ = 7.7 - 27 GeV. With upgrades on STAR detector like iTPC, higher-quality data with extended particle acceptance are collected. Figure 6 shows collision energy dependence of net-proton C_4/C_2 ($\kappa\sigma^2$) in Au+Au collisions at STAR BES energies. In the left panel of Fig. 6, new measurements are shown with red circles and red diamonds for 0-5% and 70-80% collision centrality, respectively. The measurements on BES-I datasets are shown with black open circles and diamonds [7]. Calculations from non-critical models like hydrodynamic model, HRG with a canonical ensemble, and the UrQMD model are also shown. Compared to model calculations, it can be seen that the trend of data in 0-5% central collisions can be qualitatively described by model calculations while there are quantitive differences. The right panel of Fig. 6 shows the deviations of net-proton C_4/C_2 in 0-5% central collisions as a function of collision energy from each model. It can be seen that the deviation from non-critical models reaches a maximum at $\sqrt{s_{NN}}$ = 19.6 GeV for both three models with a significance level of 4σ. The result could be the sign of the QCD critical point, but there is still a gap at low energies $3 < \sqrt{s_{NN}} < 7.7$ GeV. The measurements at these lower energies will be crucial to confirm the existence of the QCD critical point. Currently, the analysis at STAR fixed-target energies focusing on $\sqrt{s_{NN}} = 3.0 - 4.5$ GeV is ongoing. Hopefully, this measurement as well as measurements from other heavy-ion experiments at high baryon density will give a confirmative answer.

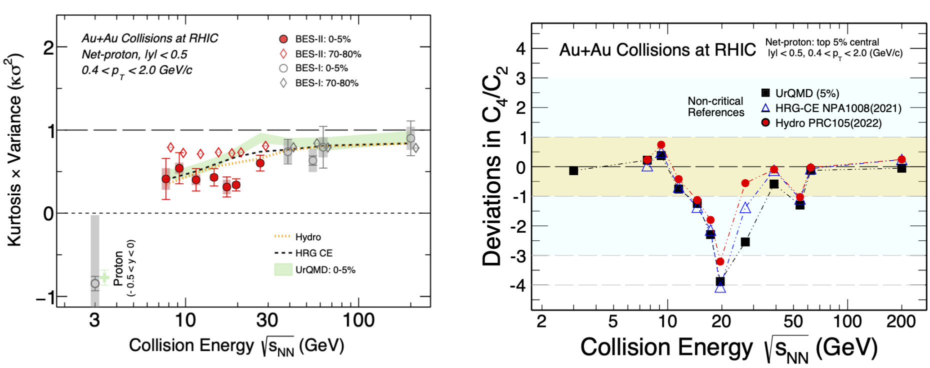

Figure 6. Left: Net-proton $\kappa\sigma^2$ as a function of collision energy ($\sqrt{s_{NN}}$) in 0-5% and 70-80% collision centrality. Right: Deviations of net-proton $\kappa\sigma^2$ from various model calculations as a function of collision energy ($\sqrt{s_{NN}}$).

6 Summary

In these proceedings, I show a brief introduction to the recent progress from experiments on the search for the QCD critical point. From various measurements, we see a maximum deviation from non-critical baselines at around 20 GeV. There could be important physics at these energies which require efforts from both experimental and theoretical sides. More important results are not shown here due to limited space.

Acknowledgements

The National Natural Science Foundation of China supported the author under No. 12305141.

References

[1] R.C. Hwa, M.T. Nazirov, Intermittency in second order phase transition, Phys. Rev. Lett. **69**, 741 (1992). 10.1103/PhysRevLett.69.741

[2] M. Abdulhamid et al. (STAR), Energy dependence of intermittency for charged hadrons in Au+Au collisions at RHIC, Phys. Lett. B **845**, 138165 (2023), 2301.11062. 10.1016/j.physletb.2023.138165

[3] K.J. Sun, L.W. Chen, C.M. Ko, J. Pu, Z. Xu, Light nuclei production as a probe of the QCD phase diagram, Phys. Lett. B **781**, 499 (2018), 1801.09382. 10.1016/j.physletb.2018.04.035

[4] M. Abdulhamid et al. (STAR), Beam Energy Dependence of Triton Production and Yield Ratio ($N_t \times N_p/N_d^2$) in Au+Au Collisions at RHIC, Phys. Rev. Lett. **130**, 202301 (2023), 2209.08058. 10.1103/PhysRevLett.130.202301

[5] V. Koch, A. Majumder, J. Randrup, Baryon-strangeness correlations: A Diagnostic of strongly interacting matter, Phys. Rev. Lett. **95**, 182301 (2005), nucl-th/0505052. 10.1103/PhysRevLett.95.182301

[6] M.A. Stephanov, Non-Gaussian fluctuations near the QCD critical point, Phys. Rev. Lett. **102**, 032301 (2009), 0809.3450. 10.1103/PhysRevLett.102.032301

[7] J. Adam et al. (STAR), Nonmonotonic Energy Dependence of Net-Proton Number Fluctuations, Phys. Rev. Lett. **126**, 092301 (2021), 2001.02852. 10.1103/PhysRevLett.126.092301